Tin oxide as stable protective layer for composite cuprous oxide water-splitting photocathodes

João Azevedo, S. David Tilley, Marcel Schreier, Morgan Stefik, Célia Sousa, João Pedro Araújo, Adélio Mendes, Michael Grätzel, Matthew T. Mayer

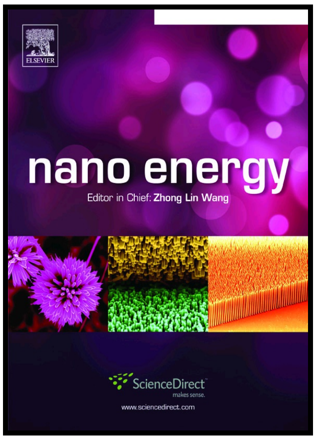

www.elsevier.com/locate/nanoenergy

PII: S2211-2855(16)30041-6
DOI: http://dx.doi.org/10.1016/j.nanoen.2016.03.022
Reference: NANOEN1200

To appear in: *Nano Energy*

Received date: 1 February 2016
Accepted date: 29 March 2016

Cite this article as: João Azevedo, S. David Tilley, Marcel Schreier, Morgar Stefik, Célia Sousa, João Pedro Araújo, Adélio Mendes, Michael Grätzel anc Matthew T. Mayer, Tin oxide as stable protective layer for composite cuprous oxide water-splitting photocathodes, *Nano Energy* http://dx.doi.org/10.1016/j.nanoen.2016.03.022

Tin Oxide as Stable Protective Layer for Composite Cuprous Oxide Water-Splitting Photocathodes

João Azevedo[a,b], S. David Tilley[c†], Marcel Schreier[c], Morgan Stefik[c‡], Célia Sousa[b], João Pedro Araújo[b], Adélio Mendes[a], Michael Grätzel[c], Matthew T. Mayer[c,]*

[a] LEPABE - Faculdade de Engenharia, Universidade do Porto, Rua Dr. Roberto Frias, 4200-465 Porto, Portugal

[b] IFIMUP and IN – Institute of Nanoscience and Nanotechnology, Departamento de Física e Astronomia, Faculdade de Ciências da Universidade do Porto, Rua do Campo Alegre, 678, 4169-007 Porto, Portugal

[c] Institut des Sciences et Ingénierie Chimiques, Ecole Polytechnique Fédérale de Lausanne, CH-1015 Lausanne, Switzerland

[†] Present address: Department of Chemistry, University of Zurich, CH-8057 Zurich, Switzerland

[‡] Present address: Department of Chemistry and Biochemistry, University of South Carolina, Columbia, South Carolina, 29208, USA

Corresponding Author

* matthew.mayer@epfl.ch / tel: +41 21 6933644 / EPFL ISIC LPI, Station 6, CH-1015 Lausanne, Switzerland

ABSTRACT: For a sustainable future, efficient solar energy harvesting and storage is required. Solar hydrogen production from photoelectrochemical water splitting is a promising technology and, in particular, cuprous oxide photocathodes are interesting photoelectrodes due to their high efficiency and low cost. However, chemical instability inhibits practical application of such devices. This work reports a novel strategy for protecting cuprous oxide from photocorrosion, wherein a thin SnO_2 overlayer enables increased stability over previous reports utilizing TiO_2 protective layers. Performance and stability are influenced by the film thickness, post-deposition steam treatment, and the nature of the heterojunction interface. Stability over 57 h of sustained photoelectrochemical water reduction, maintaining 90 % of initial photocurrent, is achieved.

KEYWORDS: water splitting, cuprous oxide, tin dioxide, stability, protective layer.

1. Introduction

Renewables inevitably will become the main power sources providing clean and local energy at a competitive price. The Sun is by far the largest power source available, illuminating the surface of the Earth with a power of 97 PW, the energy received in one day is more than humans consume in one year [1,2]. But given the intermittent nature of solar energy, efficient storage devices need to be employed in order to transform solar energy in a viable and autonomous energy source. Chemical fuels, in particular hydrogen, represent a promising way to store solar energy [3-5]. Hydrogen can be stored and later easily and efficiently converted to electricity using fuel cells [6]. Since the first report on solar water splitting [7], much research effort has been invested in developing efficient and stable photoelectrochemical (PEC) devices [8-13].

One of the most promising candidates for PEC water splitting is cuprous oxide, Cu_2O, due to its good electrical conductivity and close to optimum bandgap of 2 eV [14-16]. Although composed of naturally abundant elements, the greatest challenge is its poor stability in aqueous solutions as the reduction and oxidation of monovalent copper potentials lie between the water redox potentials [17,18]. Since unprotected Cu_2O is highly unstable, different strategies have been investigated to protect this material [19-22]. Paracchino *et al.* reported a multilayer configuration consisting of a p-n junction between p-type Cu_2O and n-type Al:ZnO (AZO) covered by a thin TiO_2 layer to prevent direct contact of the junction with the aqueous environment [17]. This configuration yielded stable photocurrents for 1 hour, upon which would decrease rapidly to near zero values. More recently, Tilley *et al.* were able to extend the stability of this photocathode by using an amorphous RuO_2 layer as a catalyst replacement for Pt [9]. This way, not only was it possible to sustain high photocurrents with ~ 100 % Faradaic efficiency but also to extend the photocathode stability up to 4 h under continuous illumination. Furthermore, in a subsequent report by the same authors, a simple steam treatment applied to the photocathode presented a ground-breaking stability enhancement, it preserved 90 % of initial photocurrent under chopped AM 1.5 illumination over 25 h (biased at 0 V_{RHE} in pH 5 electrolyte) [23].

These works proved that through improvement of the protective layers, major stability enhancements could be achieved. To be efficient, the protective layer needs to exhibit several characteristics, such as favorable energy band alignment with the Cu_2O, good electrochemical reaction rate and no corrosive side reactions should occur at potentials in the bandgap [17].

In theory, TiO_2 fulfills the necessary requirements for a good protective layer but, as observed by Paracchino *et al.*, the deposition of a TiO_2 on Cu_2O without any intermediate layer yields very low photocurrents and is highly unstable [17]. This indicates that TiO_2 does not by itself fully prevent the photocorrosion of the photocathode. Given the low photocurrent inherent to this Cu_2O/TiO_2 configuration, poor charge separation at the semiconductor interface must be promoting recombination and side reactions like Cu_2O reduction [18].

The usage of AZO provides a better interface (as evidenced by its use in heterojunction solar cells) with good charge extraction through the p-n junction between the p-type Cu_2O and n-type AZO. When annealed at 400 °C, a TiO_2 thin film shows excellent stabilities over days [24]. However, heating the Cu_2O/AZO junction over 200 °C decreases dramatically the photoelectrochemical performance [12]. A breakthrough is necessary to achieve much higher stabilities before Cu_2O photocathodes can be viable for commercial application.

The next step to enhance the stability of Cu_2O photocathodes is to implement protective layers different from the conventional TiO_2. Among semiconductors available that could conformably deposited by atomic layer deposition (ALD), tin dioxide (SnO_2) gathers all the necessary requirements. SnO_2 is a wide band gap (3.6 eV) semiconductor with a low n-type resistivity, high transparency, earth abundant and easily applicable over large surfaces [25-28]. SnO_2 has been used as protective layer in other occasions [28,29] but until now was not explored as a stand-alone protective layer for semiconductor photoelectrodes.

Here we present a simple and scalable technique for the deposition of SnO_2 for improved stability of Cu_2O photocathodes for solar water splitting. Photocurrents over -4 $mA\cdot cm^{-2}$ were achieved along with a seven-fold stability improvement over previous reports. Furthermore, different treatments and thickness were tested to further improve the stability of this composite $Cu_2O/SnO_2/RuO_2$ photocathode and the interface between materials is discussed. Stable operation under continuous illumination for 57 h, with 10 % efficiency drop used as reference, was achieved. The proposed approach has the potential to tackle the stability issue of other nonstable photoelectrodes and thus can make a significant contribution in the field of photoelectrochemical energy conversion.

2. Experimental Details

2.1 Electrodeposition of Cuprous Oxide

Samples were prepared on TEC-15 $F:SnO_2$ (FTO, NSG glass) that was previously cleaned by sonication in soapy water (15 min), acetone (15 min), ethanol (15 min) and distilled (DI) water (15 min), in that order. The substrates were then dried under a stream of compressed air gas to remove any liquid and a 10 nm chromium adhesion layer was deposited by sputtering followed by a 150 nm layer of gold. These thin layers serve as better interface for the semiconductor deposition and form a desirable ohmic contact to Cu_2O.

Galvanostatic electrodeposition was used for depositing Cu_2O because of its effectiveness, simplicity and low cost. An uncoated gold contact area was left for attaching the electrical contacts – Figure S1. The plating bath composition and deposition conditions were optimized previously [20] and a constant current density of -0.1 mA·cm^{-2} for 105 min was applied using a two-electrode configuration and platinum mesh as counter electrode, corresponding to 500 nm of semiconductor film. This thickness was confirmed by cross-sectional SEM analysis, as can be seen in Figure 1a.

2.2 Overlayer Deposition

Since Cu_2O suffers from severe photocorrosion in aqueous environments it was protected by n-type semiconductor overlayers deposited by atomic layer deposition (ALD) using a thermal ALD system (Savannah 100, Cambridge Nanotech). Prior to deposition, samples were cleaned with DI water and a small portion of the sample was covered with Kapton® tape to preserve the gold contact uncovered. Two different configurations were tested: $Cu_2O/ZnO/SnO_2/RuO_2$ and $Cu_2O/SnO_2/RuO_2$. The deposition parameters of ZnO are described in previous reports (single pulse was used in this work) [9,17]. SnO_2 was deposited at 110 °C using tetrakis(dimethylamino)tin(IV) (TDMASn, ABCR). The ALD procedure was adapted from previous reports on tin oxide [30]. The deposition was done in pulse mode under ultra pure nitrogen flow rate at 20 sccm. One single cycle of SnO_2 was made: close, 0.5 s TDMASn pulse, 10 s delay, open, 17 s delay, close, 0.015 s O_3 pulse, 10 s delay, open, 17 s delay. The growth rate was determined using spectroscopic ellipsometry (Sopra GES 5E) on samples grown on Si wafers. The range of photo energies used in the study was between 1.5 and 5.5 eV and the obtained spectra were fitted using Tauc Lorentz dispersion law (WinELI software) to extract the thickness. The growth per cycle of SnO_2 was estimated at 0.1 nm·cycle^{-1}.

2.3 Catalyst deposition

For lowering the hydrogen evolution overpotential, a catalyst is required. Ruthenium oxide (RuO_2) has been proven a good Pt substitute with greater stability [9]. RuO_2 was photoelectrochemically deposited from a 1.3 mM solution of $KRuO_4$ at a constant current density of -28.3 μA·cm^{-2} for 15 minutes under simulated one sun illumination. A light source was a 450 W Xe-lamp (Osram, ozone-free) equipped with an IR/UV filter (KG3 filter, 3 mm, Schott), calibrated with a silicon diode in order to simulate AM 1.5 illumination at 1-sun intensity across the range 300-800 nm.

2.4 Thin Film Characterization

A high-resolution scanning electron microscope (Xeiss Merlin) with a through-the-lens detector for secondary electrons was used to evaluate the morphology of the samples using an accelerating voltage of 3 kV (surface) and 5 kV (cross section). The cross section images were taken on freshly cleaved samples. The crystallinity was evaluated with a Bruker D8 Discover diffractometer, using monochromatic Cu Kα1 radiation (1.540598 Å) at a scan rate of 0.06 deg·min^{-1} with step width of 0.02°, and the Bragg reflections matched with the American Mineralogist Crystal Structure Database. Raman spectra were made using a 532 nm wavelength laser beam and were acquired with a Labram HR800 model of Jobin-Yvon Horiba spectrometer equipped with a microscope for collection of backscattered Raman signals. Phonon modes were compared with literature.

2.5 Photoelectrochemical measurements

The photoelectrode response of the photocathodes was measured in a standard three-electrode configuration using a Pt mesh as the counter electrode and an Ag/AgCl/Sat. KCl for reference electrode, connected to an Ivium Potentiostat/Galvanostat. The measurements were made in an electrolyte solution of 0.5 M Na_2SO_4 buffered with 0.1 M KH_2PO_4 to obtain pH = 5.

The photoresponse was measured under chopped irradiation using the light source described above. The scan rate for the linear sweep voltammetry was 10 $mV\cdot s^{-1}$ in the negative direction. The electrolyte was previously sparged in nitrogen and sparging was maintained during measurements to remove oxygen bubbles formed during the tests. In the long stability tests sparging was stopped to avoid electrolyte evaporation.

IPCE measurements were performed under light from a 300 W xenon lamp with integrated parabolic reflector (Cermax PE 300 BUV) passing through a monochromator (Bausch & Lomb, bandwidth 10 nm FWHM). Comparison with a calibrated Si photodiode allowed the calculation of the IPCE.

3. Results and Discussion

From the SEM image of the cross section of the photocathode (Figure 1a) it is possible to observe that the SnO_2 overlayer is 50 nm thick and the deposition is homogeneous and dense, as expected from the ALD technique. A dense overlayer is crucial for protection as it provides better isolation from the electrolyte. The Cu_2O/SnO_2 configuration with RuOx surface catalyst shows a plateau photocurrent close to -4.5 $mA\cdot cm^{-2}$ at 0 V_{RHE} with an onset at +0.34 V_{RHE} (Figure 1b), corresponding to more than twice the photocurrent reported for a TiO_2 overlayer on top of Cu_2O [17].

The stability was assessed under 1 sun illumination during 30 h (Figure 1c). The noisy photocurrent during measurement results from the hydrogen evolution at the photocathode and temporary hydrogen bubbles accumulating on the photoelectrode surface (Figure 1c onset). After 30 h biased at 0 V_{RHE}, 90 % of the photoelectrode initial photocurrent is preserved (Figure 1b). This new protective overlayer is a major improvement over previous reported results with no need for an interfacial layer. To confirm the stability of the developed photocathode, the surface of the Cu_2O/SnO_2 samples was studied in SEM images taken at different stages of the stability test. Figure 2 shows images acquired after three different durations of stability testing, no significant morphologic differences can be observed besides a slight smoothing of the RuO_x surface after 27 h.

The current-potential characteristics and stability curves of Cu_2O photocathodes coated with different SnO_2 overlayer thicknesses (20 nm, 50 nm and 100 nm) were compared (Figure S2). The samples with the 20 nm of SnO_2 show a current density decrease after the stability test of ca. 20 % and a later onset potential, whereas higher thicknesses present a higher current density and a much higher stability preserving 80 % of its initial plateau current after 45 h. These results show that SnO_2 can be optimized to improve stability by depositing thicker layers without losing performance.

The incident photon-to-current efficiency (IPCE) of the most stable photocathode (with 100 nm SnO_2) was determined, as shown in Figure S3. In the visible region between 380 and 480 nm the IPCE exceeded 40 %. Above 480 nm the IPCE values drop quickly. This behavior is in accordance with the band structure of Cu_2O. The lowest fundamental absorption transition in Cu_2O is □ (2.0 eV), at the Γ-point of the Brillouin zone, corresponding to 620 nm, which is parity forbidden [31]. The integration of the IPCE spectrum yielded 3.8 $mA \cdot cm^{-2}$, the same value obtained with the photoelectrode under simulated 1 sun illumination.

The SnO_2 layer was investigated to understand the stability improvements. The degree of crystallization was examined through XRD and Raman spectroscopy (Figure S4) and no clear indication of a SnO_2 crystalline phases in the protective layer was observed. The multilayered structure of the photocathode makes it difficult to isolate the Bragg diffraction peaks of the different materials and we hypothesize that all SnO_2 Bragg peaks identified in Figure S4a correspond actually to the FTO substrate. A grazing angle XRD (Figure S4b) was performed to eliminate the contribution from subjacent layers and also shows no sign of crystallinity, in agreement with the Raman results (Figure S4c). XRD results showed no signs of decomposition of the Cu_2O after the 30 h stability test, when compared to previous reports on unprotected samples where decomposition was observed by XRD [17].

Cross section images of the SnO_2 thin layer (Figure S5a) display a dense and crack-free coating, as expected from the ALD deposition. Although the thickness of the SnO_2 is very homogeneous a small variation is observed from the Cu_2O grain tips to the grain boundaries, typical in ALD deposition on a microcrystalline surface [23,32]. In fact, larger thicknesses at the grain boundaries and more constant thicknesses elsewhere are observed (Figure S5b). Previous reports show that a thickness variation, even small, does not offer optimum conditions for the electrodeposition of catalysts [23]. An easy way to reduce the thickness variation is by a simple low temperature steam treatment, as previously reported [23]. Three different temperatures were tested (100 ºC, 125 ºC and 150 ºC) and their performances compared by current-potential characteristics and stability tests as shown in Figure 3. No significant changes in plateau photocurrent or onset were observed, as expected, since the sample did not suffer any major morphological or structural changes. At 100 ºC there were no significant changes in stability attributed to the unaltered surface at such low temperature treatment. Nevertheless, as the steam temperature increases, the stability shows significant improvements and a maximum stability of 90 % of its initial plateau current after 57 h biased at 0 V_{RHE} was observed, with no loss in peak photocurrent or fill factor. This is a major improvement over previous reports with TiO_2 protective layer [9,17,18,23].

Predicted potential-pH phase diagrams shown in Figure S6 reveal the thermodynamic behaviors of Ti and Sn oxides under water reduction conditions. Both TiO_2 and SnO_2 are the predicted stable phases at 0 V_{RHE} in pH 5 solutions, providing little insight into the reason for the observed stability enhancement of SnO_2. For both overlayer materials, post-deposition steam treatments led to significantly improved stabilities, treatments which are believed to decrease the density of defects such as cracks and pinholes and thereby better protect the underling layers from corrosion [23]. It is therefore likely that the superior quality of ALD deposited and steam annealed SnO_2 contributed to the stability reported here. Also, better electron mobility than TiO_2 could explain less recombination and side reactions, offering better stability [28]. Further analysis of the degradation mechanisms of both device types is the topic of ongoing work. Nevertheless, we confirmed that the observed photocurrents corresponded to unity Faradaic yields for H_2 evolution, as measured by gas chromatography and presented in Figure S7.

Another aspect that can be improved in the Cu_2O/SnO_2 configuration is the interface between the active semiconductor, Cu_2O, and the protective layer, SnO_2 [17,33]. ZnO is known to provide a good interface between Cu_2O and TiO_2 probably providing a more hydroxylated surface for TiO_2 to grow on and forming a local electrostatic field at the Cu_2O/ZnO p–n junction assisting in extracting photogenerated electrons [17,18]. The significant improvements that a ZnO thin film implemented below the TiO_2 overlayer motivated us to test the same approach in the SnO_2 system. A single ALD pulse cycle of ZnO was applied between the two semiconductor layers and the samples were characterized as shown in Figure 4. The performance of the $Cu_2O/ZnO/SnO_2/RuO_2$ configuration was better with an onset at +0.55 V_{RHE} and a plateau photocurrent around -4.4 $mA \cdot cm^{-2}$ at 0 V_{RHE} (Figure 4a) showing that a single cycle of ZnO is enough to improve the interface with the protective layer. This enhanced onset over previous reports on composite Cu_2O photocathodes with RuO_2 catalyst is the same as observed with Pt catalyst [9.23.34].

When Cu_2O is exposed to atmosphere, a thin layer of CuO is spontaneously formed since it is the stable phase of copper oxide at room temperature and pressure. Deposition of ZnO onto an oxidized Cu_2O interface can reduce the CuO layer without affecting the Cu_2O underneath, thus enhancing the open-circuit voltage of devices comprised of such heterojunctions [35,36]. The effect of a single ZnO pulse cycle reported here, a positive shift in photocurrent onset potential of over 200 mV, corresponds to a significant improvement of junction photovoltage achieved without the need for the thicker Al-doped ZnO layers employed in previous reports.

The stability test of the device featuring a ZnO interlayer is shown in Figure 4b. The initial photocurrent is higher than the $Cu_2O/SnO_2/RuO_2$ device, but degradation of the current is more pronounced. This behavior is presently under further study, but an initial hypothesis is that the SnO_2 overlayer is not as conformal when deposited onto ZnO, as compared to directly onto the Cu_2O, therefore making the device more susceptible to corrosion.

4. Conclusions

In this study it was discovered that ALD deposited SnO_2 is a promising candidate overlayer for stabilizing photocathodes for hydrogen evolution. The performance and stability were influenced by the film thickness, post-deposition steam treatment, and the nature of the heterojunction interface. The optimized device exhibited great stability, maintaining 90 % of its initial photocurrent after 57 h of sustained photoelectrochemical water reduction. Further study will include identification of the mechanism of slow degradation, optimization of the heterojunctions for improved performance, and exploration of photocathode operation in acidic or alkaline solutions, which are desirable for complete devices. To the best of our knowledge, this study represents the first demonstration of SnO_2 as a photocathode protection layer [37], and these findings should be widely applicable for use on other photoelectrode devices.

5. Vitae

	**João Azevedo** obtained a master's degree in Experimental Physics at Porto University, Portugal, in 2011. Currently he is a Physics PhD candidate at Porto University and researching on solar energy storage both at LEPABE, Laboratory for Process Engineering, Environment, Biotechnology and Energy and IFIMUP-IN, Institute of Nanoscience and Nanotechnology. His research centers on the production of solar fuels, with a new photoelectrode development to improve the efficiency of water splitting processes and solar batteries.
	**S. David Tilley** obtained a PhD in chemistry from the University of California, Berkeley in 2007. Following a postdoctoral stay at Princeton University, he moved to the EPFL in Switzerland in 2009 as a postdoctoral fellow in the group of Prof. Michael Grätzel. After serving as group leader of the water splitting group in this laboratory from 2012–2014, he was appointed as tenure-track assistant professor at the University of Zurich, Switzerland, where he continues research on materials for PEC water splitting.
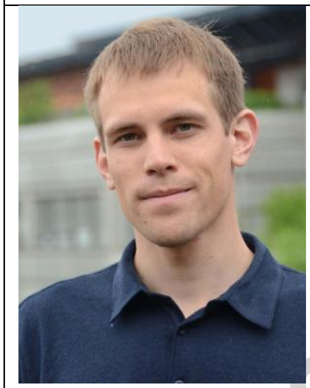	**Marcel Schreier** obtained a bachelor's degree in Chemistry and Chemical Engineering from EPFL in 2009 and a master's degree in Chemical Engineering from ETH Zurich in 2012. During his studies, he conducted research at BASF in Germany, the University of Alberta in Canada and at the California Institute of Technology. Currently, he is a PhD student in the group of Prof. Michael Grätzel at EPFL, working on the photoelectrochemical conversion of solar energy into hydrogen and carbon-based fuels.
	**Morgan Stefik** obtained a degree in Materials Engineering from Cal Poly SLO in 2005 before completing doctoral studies in Materials Science at Cornell University under Prof. U. Wiesner and Prof. F. J. DiSalvo in 2010. After two years of postdoctoral research at École Polytechnique Fédérale de Lausanne with Prof. M. Grätzel, he joined the University of South Carolina in 2013 as an Assistant Professor in the Department of Chemistry and Biochemistry. He is the founding director of the NSF supported South Carolina SAXS Collaborative. His research focuses on nanomaterials chemistry with emphasis on self-assembly techniques and atomic layer deposition.

	**Célia Sousa** is specialized in nanoscience and nanotechnology and her interdisciplinary research has been mainly focused on the fabrication of nanostructures using top-down methods for biomedical and fuel cells technological applications. She completed her PhD degree in Physics–Nanotechnology in 2011 and has an h-factor of 13, published 48 papers in international peer review journals. She is also author of an invited review article, 2 book chapters and 9 proceedings. Her research led to 3 invited talks, 23 oral presentations and 30 posters in international conferences.
	**J. P. Araújo** obtained his PhD in Physics at the University of Porto in 2002 and became Assistant Professor at the Physics and Astronomy Department at the Faculty of Sciences of University of Porto in the same year. He is now Vice-President of IFIMUP-IN, Institute of Nanoscience and Nanotechnology and counts with over 200 papers in international journals. He has relevant contributions in the field of magnetic intermetallics and oxides, and recently, in new phenomena and new technologies based on the magnetism of nanostructured materials.
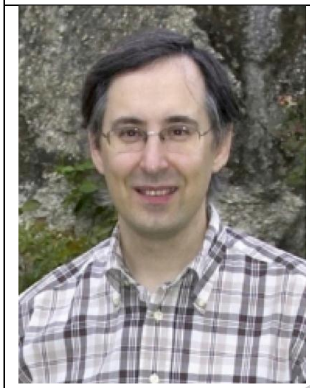	**Adélio Mendes** is full professor at FEUP and researcher at LEPABE, where he leads the Energy, Processes and Products area. His publications include over 250 papers in peer-reviewed scientific journals and 5 reviews or invited book chapters. He is the inventor or co-inventor of over 20 patents and authored one book. Prof. Mendes is presently the coordinator of project BeingEnergy (Grant agreement no: 303476), project BI-DSC (advanced research grant from ERC) and GOTSolar (Grant agreement no: 687008). He was awarded with Air Products Faculty Excellence Award (2011), ACP Diogo Vasconcelos (2011) and Solvay & Hovione Innovation Challenge 2011 (SHIC'11) prizes.
	**Michael Grätzel** is Professor of Physical Chemistry at the Ecole Polytechnique Fédérale de Lausanne, where he directs the Laboratory of Photonics and Interfaces. He pioneered research in the field of energy and electron transfer reactions in mesoscopic systems and their use for the generation of electricity and fuels from sunlight as well as the storage of electric power in lithium ion batteries. Author of several books and some 1200 publications that received over 175'000 citations (h-factor 193) he is one of the 3 most highly cited chemists in the world. His recent awards include the Paracelsus Prize of the Swiss Chemical Society, the King Feisal International Science Prize, the Samson Prime Minister's Prize for Innovation in Alternative Fuels, the First Leigh-Ann Conn Prize in Renewable Energy, the Albert Einstein World Award of Science, the Marcel Benoist Prize, the Paul Karrer

	Gold Medal, the Gutenberg Research Award, the Millennium Technology Grand Prize, and the Balzan Prize. He graduated as Doctor of natural science from the Technical University of Berlin and received 10 honorary doctors degrees from Asian and European Universities. He is a member of the Swiss Chemical Society and the German Academy of Science (Leopoldina) as well as a Honorary member of the Israeli Chemical Society, the Bulgarian Academy of Science and the Société Vaudoise de Sciences Naturelles. Recently he was named Fellow of the Max Planck Society and Honorary Fellow of the Royal Society of Chemistry (UK).
	**Matthew T. Mayer** earned a bachelor's degree in chemistry from Boise State University before completing a PhD in chemistry under Dunwei Wang at Boston College. He then joined EPFL as a postdoctoral researcher in the group of Michael Grätzel, serving as leader of the solar fuels group since 2014.

ACKNOWLEDGMENTS

J. Azevedo and C. Sousa are grateful to the FCT SFRH/BD/79207/2011 PhD grant and postdoctoral grant SFRH/BPD/82010/2011, respectively. This work was supported by research project BI-DSC (grant agreement no. 321315) funded by European Research Council and the PECHouse project (Swiss Federal Office for Energy, contract SI/500090-02). M. Schreier thanks Siemens AG for funding. M. Stefik acknowledges startup funds from the University of South Carolina. J.P. Araújo acknowledges NORTE-070124-FEDER-000070 Multifunctional Nanomaterials funded by FEDER and CCDRN.

REFERENCES

(1) G. L. Stephens, J. Li, M. Wild, C. A. Clayson, N. Loeb, S. Kato, T. L'Ecuyer, Jr P. W. Stackhouse, M. Lebsock, T. Andrews, Nat. Geosci. 5 (2012) 691-696.

(2) R. van de Krol, M. Gratzel, Photoelectrochemical Hydrogen Production, Springer Science & Business Media, New York, USA 2011.

(3) Y. Tachibana, V. Vayssieres, J. R. Durrant, Nature Photon. 6 (2012) 511-518.

(4) J. W. Jang, C. Du, Y. Ye, Y. Lin, X. Yao, J. Thorne, E. Liu, G. McMahon, J. Zhu, A. Javey, J. Guo, D. Wang, Nat. Commun. 6 (2015) 1-13.

(5) P. S.Bassi, Gurudayal, L. H. Wong, J. Barber, Phys. Chem. Chem. Phys. 16 (2014) 11834.

(6) C. A. Grimes, O. K. Varghese, S. Ranjan, Light, Water, Hydrogen: The Solar Generation of Hydrogen by Water Photoelectrolysis, Springer Science & Business Media, New York, USA 2008.

(7) A. Fujishima, K. Honda, Nature 238 (1972) 37-38.

(8) J. Y. Kim, J. W. Jang, D. H. Youn, G. Magesh, J. S. Lee, Adv. Energy Mater. 4 (2014) 1400476.

(9) S. D. Tilley, M. Schreier, J. Azevedo, M. Stefik, M. Grätzel, Adv. Funct. Mater. 24 (2014) 303-311.

(10) S. D. Tilley, M. Cornuz, K. Sivula, M. Grätzel, Angew. Chem. Int. Edit. 49 (2010) 6405-6408.

(11) M. T. Mayer, Y. Lin, G. Yuan, D. Wang, Acc. Chem. Res. 46 (2013) 1558-1566.

(12) G. Wang, H. Wang, Y. Ling, Y. Tang, X. Yang, R. C. Fitzmorris, C. Wang, J. Z. Zhang, Y. Li, Nano Lett. 11 (2011) 3026-3033.

(13) F. Lin, S. W. Boettcher, Nat Mater. 13 (2013) 81–86.

(14) D. Barreca, P. Fornasiero, A. Gasparotto, V. Gombac, C. Maccato, T. Montini, E. Tondello, ChemSusChem 2 (2009) 230-233.

(15) C. M. McShane, K. S. Choi, Phys. Chem. Chem. Phys. 14 (2012) 6112-6118.

(16) M. Hara, T. Kondo, M. Komoda, S. Ikeda, J. N. Kondo, K. Domen, M. Hara, K. Shinohara, A. Tanaka, Chem. Commun. (1998) 357-358.

(17) A. Paracchino, V. Laporte, K. Sivula, M. Grätzel, E. Thimsen, Nat. Mater. 10 (2011) 456-461.

(18) A. Paracchino, N. Mathews, T. Hisatomi, M. Stefik, S. D. Tilley, M. Grätzel, Energy Environ. Sci. 5 (2012) 8673-8681.

(19) Z. Zhang, P. Wang, J. Mater. Chem. 22 (2012) 2456-2464.

(20) A. Paracchino, J. C. Brauer, J. E. Moser, E. Thimsen, M. Grätzel, J. Phys. Chem. C 116 (2012) 7341-7350.

(21) Y. Mao, J. He, X. Sun, W. Li, X. Lu, J. Gan, Z. Liu, L. Gong, J. Chen, P. Liu, Y. Tong, Electrochim. Acta 62 (2012) 1-7.

(22) M. Wang, L. Sun, Z. Lin, J. Cai, K. Xie, C. Lin, Energy Environ. Sci. 6 (2013) 1211-1220.

(23) J. Azevedo, L. Steier, P. Dias, M. Stefik, C. T. Sousa, J. P. Araujo, A. Mendes, M. Grätzel, S. D. Tilley, Energy Environ. Sci. 7 (2014) 4044-4052.

(24) B. Seger, S. D. Tilley, T. Pedersen, P. C. K. Vesborg, O. Hansen, M. Grätzel, I. Chorkendorff, RSC Adv. 3 (2013) 25902-25907.

(25) S. J. Ikhmayies, Int. J. Mat. Chem. 2 (2012)173-177.

(26) L. Tan, L. Wang, Y. Wang, J. Nanomater. 2011 (2011) 1-10.

(27) M. A. Yıldırım, Y. Akaltun, A. Ateş, Solid State Sci. 14 (2012) 1282-1288.

(28) J. Hu, Y. F. Zhu, Q. Liu, Y. B. Gao, R. G. Du, C. J. Lin, J. Electrochem. Soc. 162 (2015)

C161–C166.

(29) M. G. Kast, L. J. Enman, N. J. Gurnon, A. Nadarajah, S. W. Boettcher, ACS Appl. Mater. Interfaces. 6 (2014) 22830–22837.

(30) M. Stefik, M. Cornuz, N. Mathews, T. Hisatomi, S. Mhaisalkar, M. Grätzel, Nano Lett. 12 (2012) 5431-5435.

(31) B. K. Meyer, A. Polity, D. Reppin, M. Becker, P. Hering, P. J. Klar, T. Sander, C. Reindl, J. Benz, M. Eickhoff, C. Heiliger, M. Heinemann, J. Bläsing, A. Krost, S. Shokovets, C. Müller, C. Ronning, Phys. Status Solidi B 249 (2012) 1487-1509.

(32) K. Murakami, M. Rommel, B. Hudec, A. Rosová, K. Hušeková, E. Dobročka, R. Rammula, A. Kasikov, J. H. Han, W. Lee, S. J. Song, A. Paskaleva, A. J. Bauer, L. Frey, K. Fröhlich, J. Aarik, C. S. Hwang, ACS Appl. Mater. Interfaces 6 (2014) 2486-2492.

(33) P. Dai, W. Li, J. Xie, Y. He, J. Thorne, G. McMahon, J. Zhan, D. Wang, Angew. Chem. Int. Edit. 53 (2014) 13493-13497.

(34) C. G. Morales-Guio, S. D. Tilley, H. Vrubel, M. Grätzel, X. Hu, Nat. Commun. 5 (2014) 3059.

(35) S. S. Wilson, J. P. Bosco, Y. Tolstova, D. O. Scanlon, G. W. Watson, H. A. Atwater, Energy Environ. Sci. 7 (2014) 3606-3610.

(36) Y. S. Lee, D. Chua, R. E. Brandt, S. C. Siah, J. V. Lim, J. P. Mailoa, S. W. Lee, R. G. Gordon, T. Buonassisi, Adv. Mater. 26 (2014) 4704-4710.

(37) S. Hu, N. S. Lewis, J. W. Ager, J. Yang, J. R. Mckone, N. C. Strandwitz, J. Phys. Chem. C 119 (2015) 24201-24228.

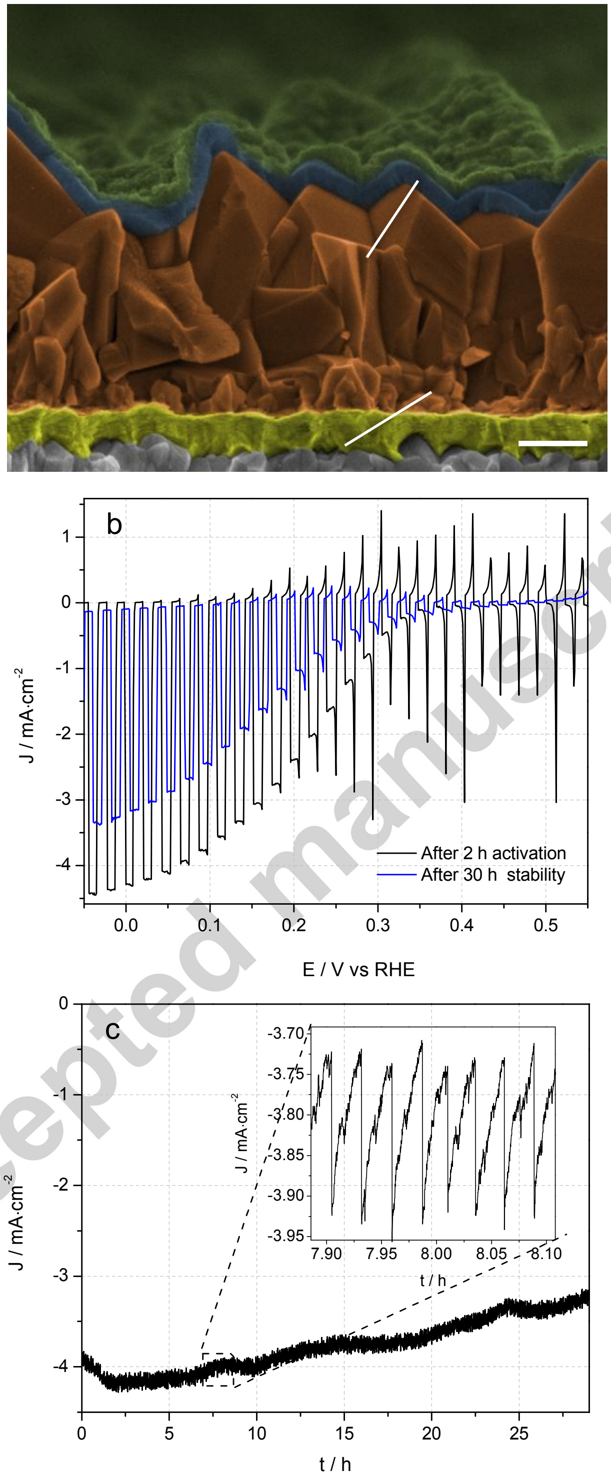

Figure 1. (a) Cross-sectional SEM image of a photocathode showing the respective layer thicknesses. (b) Current-potential characteristics of a composite $Cu_2O/SnO_2/RuO_2$ photocathode under chopped simulated sunlight illumination, acquired after 2 h activation and after 30 h

stability measurement (depicted in (c)). (c) Chronoamperometric stability measurement under 0 V_{RHE} bias and continuous illumination. The inset shows small fluctuations in the measured current due to gas bubble evolution, trapping (loss of surface area), and eventual escape (surface area recovered).

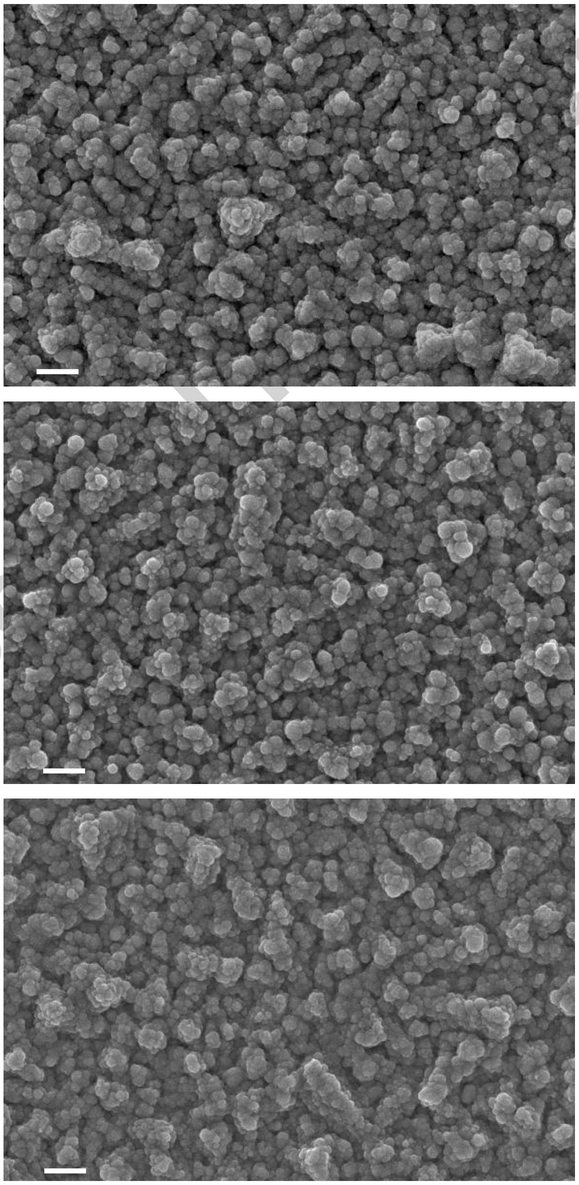

Figure 2. SEM top view of a photocathode with photo-assisted electrodeposited RuO_2 catalyst (a) as deposited, (b) after 3 h and (c) 27 h under illumination at 0 V_{RHE} bias.

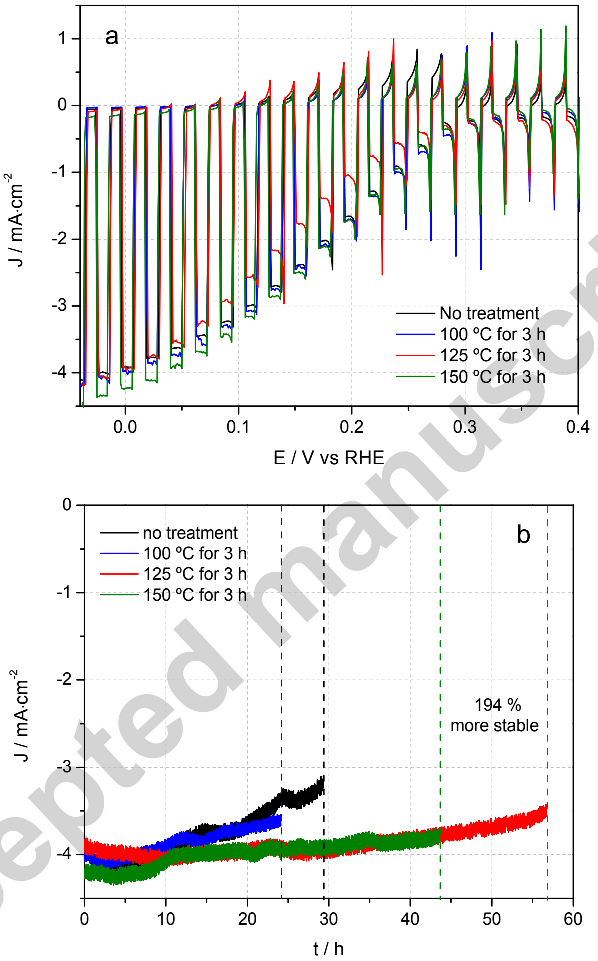

Figure 3. (a) Current-potential characteristics of composite $Cu_2O/SnO_2/RuO_2$ photocathode samples with different steam treatment conditions: without treatment and with 3 h steam treatment at temperatures of 100, 125 and 150 ºC. (b) Corresponding stability measurements under continuous illumination while biased at 0 V_{RHE}. All measurements were carried out in pH 5.0 phosphate–sulfate electrolyte.

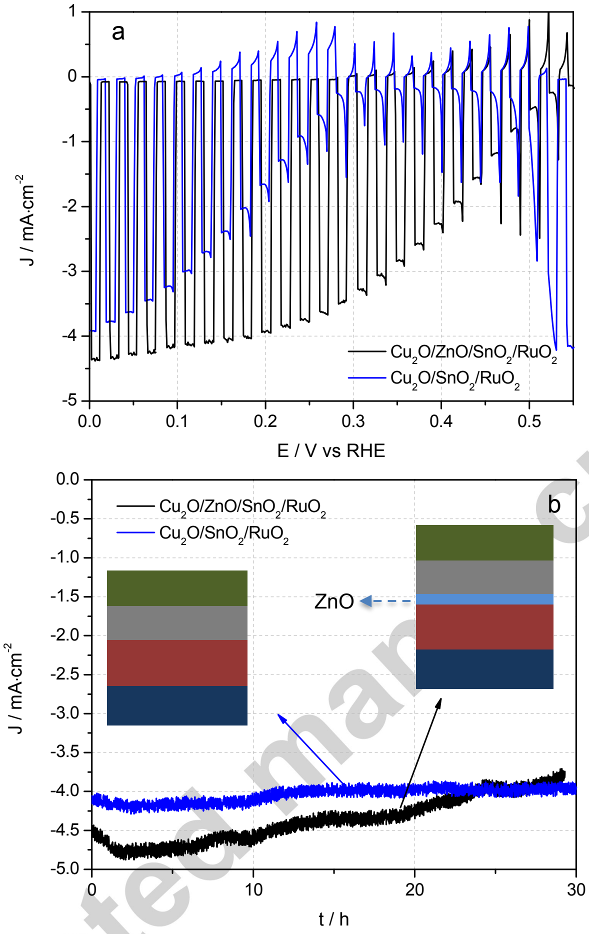

Figure 4. Photoelectrochemical characteristics of composite photocathodes. (a) Current-potential comparison between the performance of a photocathode with ($Cu_2O/ZnO/SnO_2/RuO_2$) and without ($Cu_2O/SnO_2/RuO_2$) ZnO layer. (b) Chronoamperometric stability measurements under continuous illumination while biased at 0 V_{RHE}. All measurements were carried out in pH 5.0 phosphate–sulfate electrolyte.

Highlights

- Report a new protective overlayer for Cu_2O with enhanced chemical stability that should be broadly applicable to other photocathode materials
- Optimized photocathodes were stable over 57 h of continuous illumination (twice as much as previous reported works), an important advance among Cu_2O-based devices
- Studied influence of an interlayer of ZnO between Cu_2O and the protective layer and achieved improved onset potential
- Applied a steam treatment, previously reported for TiO_2, and here demonstrated that can be used for other materials with similar improvements